MATHEMATICAL MODELLING AND ANALYSIS
VOLUME 9 NUMBER 2, 2004, PAGES 99-114 ©
2004 Technika ISSN 1392-6292

NUMERICAL SIMULATION OF UNSTEADY TWO-LAYERED PULSATILE BLOOD FLOW IN A STENOSED FLEXIBLE ARTERY: EFFECT OF PERIPHERAL LAYER VISCOSITY [1]

S. CHAKRAVARTY[1], P. K. MANDAL[2] and A. MANDAL[1]

[1] *Department of Mathematics*

Visva-Bharati University, Santiniketan 731 235, INDIA E-mail: dgp_santbrat@sancharnet. in

[2] *Department of Mathematics, Krishnath College*

P.O.-Berhampore, Dt.- Murshidabad, W.B., INDIA

E-mail: pkmind02@yahoo. co. uk

Received December 13, 2003; revised April 20, 2004

Abstract. The present paper deals with a theoretical investigation of blood flow in an arterial segment in the presence of stenosis. The streaming blood is treated to be composed of two different layers - the central core and the plasma. The former is considered to be non-Newtonian liquid characterised by the *Power law* model, while the latter is chosen to be Newtonian. The artery is simulated as an elastic (moving wall) cylindrical tube. The unsteady flow mechanism of the present study is subjected to a pulsatile pressure gradient arising from the normal functioning of the heart. The time-variant geometry of the stenosis has been accounted for in order to improve resemblance to the real situation. The unsteady flow mechanism, subjected to pulsatile pressure gradient, has been solved using finite difference scheme by exploiting the physically realistic prescribed conditions. An extensive quantitative analysis has been performed through numerical computations of the flow velocity, the flux, the resistive impedances and the wall shear stresses, together with their dependence with the time, the input pressure gradient and the severity of the stenosis, presented graphically at the end of the paper in order to illustrate the applicability of the model under consideration. Special emphasis has been made to compare the existing results with the present ones and found to have a good agreement. Key words: Moving wall, non-Newtonian liquids, stenosis, power-law

[1] The authors would like to thank the referees for careful reading for the manuscript and for helpful suggestions

1. Introduction

The studies related to blood flow through stenosed arteries have wide implications as the most serious physiological problems causing circulatory diseases associated with disturbed flow conditions in the arterial system. Partial occlusion of a blood vessel due to abnormal and unnatural growth of tissue, usually referred to as a stenosis, is one of the most frequently occurring abnormalities in the cardiovascular system. It results from flow disorder with a considerable reduction of the transportation of blood to the region beyond the arterial constriction. Although the root cause of the formation of arterial constriction is not completely understood by the theoretical modelers, but its effect on the flow phenomena does have serious consequences. The normal circulation gets disrupted to the extent depending upon the severity of the stenosis. Under normal physiological condition, the transport of blood in the human circulatory system depends entirely on the pumping action of the heart producing a pressure gradient throughout the arterial system.

For the purpose of a clear understanding of the development of stenosis from the physical point of view one needs to be fully conversant with the haemodynamic characteristics of the flowing blood together with the mechanical properties of the vascular wall material under physiological conditions. Several analytical studies dealing with blood flow through stenosed arteries have been carried out in the recent past [10, 13, 23, 24] with the assumption that the flow of blood to be Newtonian and the stenosis be represented by a mathematical function viz. the cosine function. However, experimental investigations reveal that blood, being a suspension of cells, behaves like a non-Newtonian fluid at a low shear rates in smaller arteries [4, 5, 17]. All these studies recorded the flowing blood to be a homogeneous fluid although blood is composed of a complex acquous continuous phase with numerous cells or corpuscles of different kinds suspended in it. The consideration of a homogeneous fluid as a representative of the flowing blood thus simplifies the relevant problem to a great extent.

Some researchers [1, 7, 21] have shown that for blood flowing through small vessels there is an erythrocyte-free plasma (Newtonian) layer adjacent to the vessel wall and a core layer of suspension of all the erythrocytes (non-Newtonian). Accepting this idea, several studies [6, 8, 14, 15, 16, 18, 19] revealed that the existence of the peripheral layer would be of some significance in functioning of the diseased arterial system. In most of the recent literatures relevant to stenotic flow cither in a rigid tube or in a flexible artery, the stenotic geometry has been regarded largely as time-independent. Such assumption may suit well for a rigid vessel but for a flexible one, the stenosis cannot remain static. Very recently, a study on two-layered model of pulsatile blood flow through stenotic blood vessels where the streaming blood in the core region was considered as a inhomogeneous Newtonian fluid, has been successfully carried out by Mandal [11] using finite difference technique. Therefore, for a realistic description of blood flow in a stenosed artery, perhaps it would be most appropriate to treat blood as a two-fluid model consisting of a central core region containing all the erythrocytes assumed to be a non-Newtonian fluid and a peripheral layer of plasma as a Newtonian fluid while the vessel is treated as a deformable one. An improved problem such as this should include the two-dimensional flow charac-

teristics of blood in order to have a complete understanding of the flow disorder in the presence of stenosis.

With the above discussion in mind, an attempt is made in the present theoretical study to examine some of the important characteristics of the blood flow through a stenosed flexible artery under a pulsatile pressure gradient. This study considers the arterial segment to be an elastic cylindrical tube containing a nonhomogeneous fluid representing blood. Blood is assumed to be composed of two different layers viz. the central core and the plasma. The former is considered to be non-Newtonian (where the blood cells are aggregated most) characterised by the Power law model while the latter (free from cells of any kind) is treated to be Newtonian. Special emphasis has been put on the effect of a suitable time-variant geometry of the stenosis in order to have the dynamic response of the stenosed arterial system under consideration. Although the general problem such as this is of great concern, due attention is also paid to the effect of the vascular wall motion on local fluid mechanics but not on the stresses and strains in the arterial wall. The cylindrical coordinate system has been taken for the analytical formulation. The governing equations of motion for the system supplemented by the appropriate boundary conditions are solved numerically, following a radial coordinate transformation, using a suitable finite difference scheme. This scheme bears the potential to perform a thorough quantitative analysis for the desired quantities through the exhibition of their results graphically followed by an exhaustive discussion so as to justify the applicability of the present study.

2. Formulation of the Problem

The stenosed arterial segment under consideration is simulated as a thin elastic cylindrical tube containing a nonhomogeneous fluid consisting of Newtonian and a non-Newtonian fluids representing the plasma and the central core of the blood respectively. The non-Newtonian core fluid is characterised by the Power law fluid with a viscosity as a function of shear rate. Let (r, *0, z)* be the coordinates of a material point in the cylindrical polar coordinate system where the z-axis is taken along the axis of the artery while r, *0* are taken along the radial and the circumferential directions respectively. The geometry of the time-dependent stenosis (cf. Figure 1) is described mathematically as

$$\frac{(R, R_1)(z,t)}{a} = \begin{cases} \left[(1, \xi_\beta) - \dfrac{(\tau_m, \delta_m)}{a l_0^2}\left\{l_0(z-d) - (z-d)^2\right\}\right] a_1(t), \\ \qquad\qquad\qquad\qquad\qquad\qquad d \le z \le d + l_0, \\ (1, \xi_\beta) a_1(t), \qquad\qquad\qquad\qquad \text{otherwise}, \end{cases}$$

where $R(z,t)$ is the radius of the arterial segment in the constricted region, a the constant radius of the normal artery outside the stenotic region, l_0 the length of the stenosis, d the location of the stenosis and (τ_m, δ_m) are the maximum heights of the stenosis and bulging of interface respectively appearing at $z = d + l_0/2$ where $\delta_m = \xi_\beta \tau_m$. Here $R_1(z,t)$ is chosen to be the radius of the central core layer and a peripheral plasma layer of thickness $(R - R_1)$ as shown in Figure 1. The time-variant parameter $a_1(t)$ is given by

$$a_1(t) = 1 - b(\cos\omega t - 1)e^{-b\omega t},$$

in which *w* represents the angular frequency and *b* is a constant. The arterial segment under consideration is chosen to be of finite length *L*.

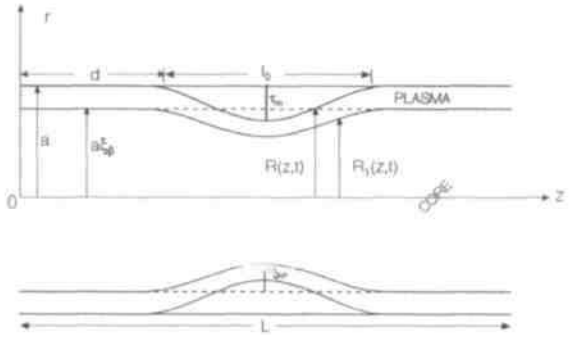

Figure 1. Geometry of the arterial stenosis with peripheral layer

Since the elastic arteries have high wave velocity (typically 5000-10000 m/sec.) due to the pulsatile nature of the streaming blood as evident from [3], this results in long wave lengths (about 10 times the length of the aorta at the fundamental cardiac frequency), small axial and radial convective acceleration and very small axial diffusion of momentum at axial distances far from the entrance of the arterial tube [22]. Keeping in view of these simplifying assumptions and considering the stenotic blood flow to be axisymmetric, laminar, one-dimensional and fully developed, the basic equation of motion governing the unsteady flow in the absence of any radial and rotational flow may be written as

$$\rho\frac{\partial w_i}{\partial t} + \frac{1}{r}\frac{\partial}{\partial r}\left[r(\tau_{rz})_i\right] = -\frac{\partial p}{\partial z}, \quad i = 1, 2, \tag{2.1}$$

where $w_i = w_i$ (r, *z, t)* is the axial flow velocity for the central (r = 1) and for the plasma (r = 2), *p* the pressure, *p* the density. The shear stress (τ_{rz})i (*i* = 1,2) for the central core and the plasma are described by

$$(\tau_{rz})_1 = \mu_1\epsilon_1^n, \qquad 0 \le r \le R_1(z,t) \quad \text{(central core)}, \tag{2.2}$$

$$(\tau_{rz})_2 = \mu_2\epsilon_2, \qquad R_1(z,t) \le r \le R(z,t) \ \text{(plasma)}, \tag{2.3}$$

with μ_1 representing the viscosity of the core fluid consisting of most of the blood cells, *n* the non-Newtonian parameter of the Power law model, μ_2 the viscosity of the plasma adjacent to the vessel wall and ϵ_1 , ϵ_2 being the respective strain rates. Since the flow is considered only in the axial direction, we further have

$$\frac{\partial p}{\partial r} = 0, \quad \frac{\partial p}{\partial \theta} = 0. \tag{2.4}$$

The above equations (2.1) and (2.4) governing blood flow have been derived with the introduction of the equation of continuity for the axial flow only. These relations

yield $p = p(z, t)$. Further we represent the pumping action of the heart by the pressure gradient $\frac{\partial p}{\partial z}$ present in (2.1) produced by it, the form of which has been taken from [2] for human being as

$$-\frac{\partial p}{\partial z} = A_0 + A_1 \cos \omega t, \tag{2.5}$$

where A_0 is the constant amplitude of the pressure gradient, A_1 is the amplitude of the pulsatile component giving rise to systolic and diastolic pressure; $\Omega = 2\pi f_p$, f_p is the pulse frequency.

3. Boundary and Initial Conditions

The velocity gradient of the core flow along the axis of the artery may be assumed to be equal to zero; that means, there is no shear rate of the core fluid along the axis which may be written as

$$\frac{\partial w_1}{\partial r} = 0 \quad \text{on } r = 0. \tag{3.1}$$

Also, at the interface of the plasma and the central core of blood media, the velocities and the stresses are assumed to be continuous which may be expressed mathematically as

$$w_1 = w_2 \qquad \text{on } r = R_1(z,t), \tag{3.2}$$

$$(\tau_{rz})_1 = (\tau_{rz})_2 \quad \text{on } r = R_1(z,t). \tag{3.3}$$

Further considering that the plasma particles adhere to the arterial wall surface, the axial velocity of the plasma particles on the wall surface may be taken to be the usual no-slip condition, given by

$$w_2 = 0 \quad \text{on } r = R(z,t). \tag{3.4}$$

Here Ω_1 , Ω_2 are the respective velocities of the central core and the plasma fluid of the non-Newtonian flowing blood and $R_1(z,t)$,$R(z,t)$ represent the respective boundaries for the central core and the plasma adhere to the arterial wall.

Rather than starting the calculation from a zero flow field, an initial condition consistent with the above boundary and interface conditions has to be chosen. To develop the initial velocities, we have made use of the basic principle of steady flow together with the relation for a constant pressure gradient p. By exploiting appropriate boundary and interface conditions an integration gives the equation (3.5) and thus the starting flow velocities of the core and plasma fluids at $t = 0$ can be written as

$$\begin{aligned} w_1(r,z,0) &= \left(\frac{p}{2\mu_1}\right)^{1/n}\left(\frac{n}{n+1}\right)\left[R_1(z,0)^{\frac{n+1}{n}} - r^{\frac{n+1}{n}}\right] \\ &\quad + \left(\frac{A_0+A_1}{4\mu_2}\right)\left[R^2(z,0) - r^2\right], \quad 0 \le r \le R_1(z,0), \\ w_2(r,z,0) &= \left(\frac{A_0+A_1}{4\mu_2}\right)\left[R^2(z,0) - r^2\right], \quad R_1(z,0) \le r \le R(z,0). \end{aligned} \tag{3.5}$$

4. Method of Solution

Introducing the constitutive relations (2.2) and (2.3) into (2.1), the equations governing blood flow in the central core and the plasma may be written as

$$\begin{cases} \dfrac{\partial w_1}{\partial t} = -\dfrac{1}{\rho}\dfrac{\partial p}{\partial z} - \dfrac{(-1)^n \mu_1}{\rho}\left[n\left(\dfrac{\partial w_1}{\partial r}\right)^{n-1}\dfrac{\partial^2 w_1}{\partial r^2} + \dfrac{1}{r}\left(\dfrac{\partial w_1}{\partial r}\right)^n\right], \\ \qquad\qquad 0 \le r \le R_1(z,t), \\ \dfrac{\partial w_2}{\partial t} = -\dfrac{1}{\rho}\dfrac{\partial p}{\partial z} + \dfrac{\mu_2}{\rho}\left[\dfrac{\partial^2 w_2}{\partial r^2} + \dfrac{1}{r}\dfrac{\partial w_2}{\partial r}\right], \qquad R_1(z,t) \le r \le R(z,t). \end{cases} \tag{4.1}$$

Usually in a problem involving coupling of the fluid mechanics with the arterial wall mechanics, *R(z,t)* would not be given but instead, could be computed as a part of the solution of the coupled problem. The nresent analysis provides *R(z, t)* with its explicit form and hence the entire attention has been focused on the haemodynamic factors only.

Let us introduce a radial coordinate transformation, given by $\xi = \dfrac{r}{R(z,t)}$ which has the effect of immobilizing the arterial wall in the transformed coordinate ξ. Using this transformation, the equations (4.1) take the following form

$$\begin{cases} \dfrac{\partial w_1}{\partial t} = -\dfrac{1}{\rho}\dfrac{\partial p}{\partial z} + \dfrac{\mu_1}{\rho R^2}\left(-\dfrac{1}{R}\dfrac{\partial w_1}{\partial \xi}\right)^{n-1}\left[n\dfrac{\partial^2 w_1}{\partial \xi^2} + \dfrac{1}{\xi}\dfrac{\partial w_1}{\partial \xi}\right] \\ \qquad\qquad + \dfrac{\xi}{R}\dfrac{\partial R}{\partial t}\dfrac{\partial w_1}{\partial \xi}, \quad 0 \le \xi \le \xi_\beta, \\ \dfrac{\partial w_2}{\partial t} = -\dfrac{1}{\rho}\dfrac{\partial p}{\partial z} + \dfrac{\mu_2}{\rho R^2}\left[\dfrac{\partial^2 w_2}{\partial \xi^2} + \dfrac{1}{\xi}\dfrac{\partial w_2}{\partial \xi}\right] + \dfrac{\xi}{R}\dfrac{\partial R}{\partial t}\dfrac{\partial w_2}{\partial \xi}, \quad \xi_\beta \le \xi \le 1, \end{cases} \tag{4.2}$$

with

$$\xi_\beta = \frac{R_1(z,t)}{R(z,t)}, \quad w_i = w_i(\xi, z, t), \quad i = 1, 2.$$

The boundary conditions (3.1)- (3.4) are transformed to

$$\begin{cases} \dfrac{\partial w_1}{\partial \xi} = 0 \quad \text{on } \xi = 0, \\ w_1 = w_2 \quad \text{on } \xi = \xi_\beta, \\ \dfrac{1}{R^{n-1}}\dfrac{\mu_1}{\mu_2}\left(-\dfrac{\partial w_1}{\partial \xi}\right)^n = -\dfrac{\partial w_2}{\partial \xi} \quad \text{on } \xi = \xi_\beta, \\ w_2(\xi, z, t) = 0 \quad \text{on } \xi = 1, \end{cases} \tag{4.3}$$

while the initial conditions (3.5) to

$$\begin{aligned} w_1(\xi, z, 0) &= \left(\frac{A_0 + A_1}{2\mu_1}\right)^{1/n}\left(\frac{n}{n+1}\right)\left(\xi_\beta^{\frac{n+1}{n}} - \xi^{\frac{n+1}{n}}\right)R^{\frac{n+1}{n}}(z,0) \\ &\quad + \left(\frac{A_0 + A_1}{4\mu_2}\right)\left[1 - \xi_\beta^2\right]R^2(z,0), \quad 0 \le \xi \le \xi_\beta, \\ w_2(\xi, z, 0) &= \left(\frac{A_0 + A_1}{4\mu_2}\right)R^2(z,0)\left[1 - \xi^2\right], \quad \xi_\beta \le \xi \le 1. \end{aligned} \tag{4.4}$$

5. Finite Difference Approximations

The finite difference scheme for solving the equations (4.2) is based on the central difference formula in order to transform all the spatial derivatives in the following manner:

with $\Delta = \Delta_\xi$ for $0 \le \xi \le \xi_\beta$ and $\Delta = \Delta_{\xi'}$ for $\xi_\beta \le \xi \le 1$,

$$\frac{\partial^2 w_m}{\partial \xi^2} = \frac{(w_m)^k_{i+1,j} - 2(w_m)^k_{i,j} + (w_m)^k_{i-1,j}}{\Delta^2} = (w_{m\,s\xi})^k_{i,j},$$

while the time derivatives are transformed by their forward difference approximations given by

$$\frac{\partial w_m}{\partial t} = \frac{(w_m)^{k+1}_{i,j} - (w_m)^k_{i,j}}{\Delta t},$$

for $m = 1, 2$. Here $w_m(\xi, z, t)$ is discretised to $w_m(\xi_i, z_j, t_k)$ and in turn, to $(w_m)^k_{i,j}$, where we define $\xi_i = (i-1)\Delta_\xi$ for $0 \le \xi \le \xi_\beta$ and $\xi_i = (i-1)\Delta_{\xi'}$ for $\xi_\beta \le \xi \le 1$, $i = 1, 2, \ldots N+1$, $z_j = (j-1)\Delta_z$, $j = 1, 2, \ldots M+1$ and $t_k = (k-1)\Delta_t$, $k = 1, 2, \ldots$ for the entire arterial segment under study, $\Delta_\xi, \Delta_{\xi'}$ are the respective increments in the radial direction for both the core and the plasma regions, while Δ_z is that along the axial direction and Δ_t is the time increment.

We replace the spatial and time derivatives in (4.2) by the finite difference representations so that differential equations may be transformed to the following difference equations:

$$(w_1)^{k+1}_{i,j} = (w_1)^k_{i,j} + \Delta_t\Big[-\frac{1}{\rho}(\frac{\partial p}{\partial z})^k + \frac{\mu_1}{\rho(R^k_j)^2}\Big| - \frac{1}{R^k_j}(w_{1\,f\xi})^k_{i,j}\Big|^{n-1} \tag{5.1}$$
$$\times\Big(n(w_{1\,s\xi})^k_{i,j} + \frac{1}{\xi_i}(w_{1\,f\xi})^k_{i,j}\Big) + \frac{\xi_i}{R^k_j}\Big(\frac{\partial R}{\partial t}\Big)^k_j (w_{1\,f\xi})^k_{i,j}\Big], \quad 0 \le \xi \le \xi_\beta$$

$$(w_2)^{k+1}_{i,j} = (w_2)^k_{i,j} + \Delta_t\Big[-\frac{1}{\rho}(\frac{\partial p}{\partial z})^k + \frac{\mu_2}{\rho(R^k_j)^2}(w_{2\,s\xi})^k_{i,j} \tag{5.2}$$
$$+ \frac{1}{\xi_i}(w_{2\,f\xi})^k_{i,j}\frac{\xi_i}{R^k_j}\Big(\frac{\partial R}{\partial t}\Big)^k_j (w_{2\,f\xi})^k_{i,j}\Big], \quad \xi_\beta \le \xi \le 1,$$

where the notations $(\,)$, $(\,)$ and $(\,)^k$ indicate that in the expressions, ξ, z, t are replaced by ξ_i, z_j, t_k respectively, wherever they appear.

Also the boundary conditions and the initial conditions have their finite difference representations, given by

$$\begin{cases} (w_1)^k_{1,j} = (w_1)^k_{2,j}, \quad (w_1)^k_{\beta,j} = (w_2)^k_{\beta,j}, \quad j = 1(1)M+1, \\ (w_2)^k_{\beta+1,j} = (w_1)^k_{\beta,j} - \frac{\mu_1}{\mu_2}\frac{\Delta_{\xi'}}{(R^k_j)^{n-1}}\left[\frac{(w_1)^k_{\beta-1,j}-(w_1)^k_{\beta,j}}{\Delta_\xi}\right]^n, \\ (w_2)^k_{N+1,j} = 0, \\ (w_1)^1_{i,j} = \left(\frac{A_0+A_1}{2\mu_1}\right)^{1/n}\left(\frac{n}{n+1}\right)\left(\xi_\beta{}^{\frac{n+1}{n}} - \xi_i^{\frac{n+1}{n}}\right)\left(R^1_j\right)^{\frac{n+1}{n}} \\ \qquad\qquad + \left(\frac{A_0+A_1}{4\mu_2}\right)\left[1-\xi^2_\beta\right]\left(R^1_j\right)^2, \\ (w_2)^1_{i,j} = \left(\frac{A_0+A_1}{4\mu_2}\right)\left(R^1_j\right)^2\left[1-\xi_i{}^2\right], \end{cases} \tag{5.3}$$

where the index β corresponds to $\xi = \xi_\beta$.

The difference equations (5.1) and (5.2) are solved for w_1 and w_2. by making use of the stated conditions (5.3) throughout the arterial segment under consideration. After having obtained the flow velocities for both the central core and the plasma, the volumetric flow rate *(Q),* the resistance to flow (r_{rz}) and the wall shear stress (r_{rz}) can be determined as

$$Q = 2\pi R^2\left[\int^{\xi_\beta}\xi w_1\, d\xi + \int^1 \xi w_2\, d\xi\right], \quad \lambda = \frac{|z_{M+1}\dfrac{\partial p}{\partial z}|}{Q}$$

$$Q' = \frac{Q}{Q_n}, \quad \lambda' = \frac{\lambda}{\lambda_n}, \quad \tau' = \frac{\tau}{\tau_n},$$

$$\tau_{rz} = \frac{\mu_1}{\quad}$$

where Q_n, λ_n and τ_n are the flux, the resistance to flow and wall shear stress, respectively, for the normal artery in the absence of peripheral layer.

$$(\tau_{rz})^k_j = \frac{\mu_1}{\Delta_\xi (R^k_j)^n}[(w_1)^k_{\beta-1,j} - (w_1)^k_{\beta,j}] + \frac{\mu_2}{\Delta_{\xi'} R^k_j}(w_2)^k_{N,j}.$$

Finally, the expressions for the dimensionless flux (Q'), resistance to flow (A') and wall shear stress (r') are given as

6. Numerical Results and Discussion

We have undertaken a specific numerical illustration using the available experimental data for the various physical parameters involved in the present analysis in order to examine the validity of the mathematical model under consideration. For the purpose of numerical computation of the desired quantities.the following input data have been made use of [1,2, 12,20]:

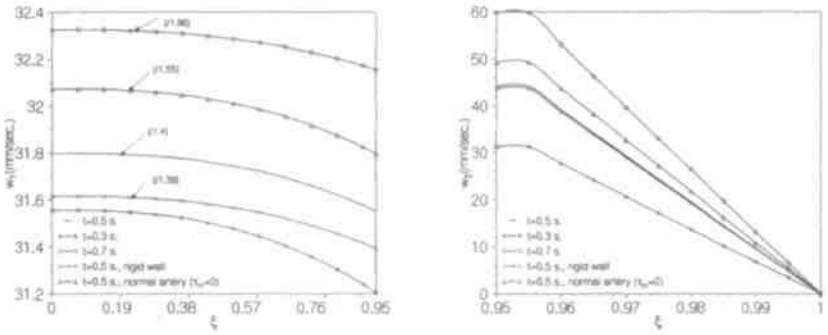

a) b)

Figure 2. Velocity profile for the flow at $z = 15\,mm$ ($\tau_m = 0.2a, \xi_\beta = 0.95,\ n = 0.639$) : a) w_1 function, b) w_2 function.

$a = 1.52$ mm, $l_0 = 15$ mm, $d = 7.5$ mm, $L = 30$ mm, $b = 0.1$,
$\rho = 1.05 \times 10^3$ kgm^{-3}, $f_p = 1.2$ Hz, $A_0 = 100$ kgm^{-2}s^{-2}, $A_1 = 0.2A_0$,
$\xi_\beta = 0.95$, $n = 0.639$, $\Delta_\xi = 0.019$, $\Delta_z = 0.15$, $\Delta_{\xi'} = 0.0025$, $\tau_m = 0.2a$.

The explicit difference scheme has been found to be quite effective for solving equations (5.1), (5.2) numerically for different time periods. The results have converged with an accuracy of the order $\sim 10^{-8}$ when the time step was chosen to be 0.000001.

Numerical results computed through the use of the above-mentioned data for various quantities of interest in order to estimate them quantitatively, are exhibited through Figs. 2 – 6. The results of the present analysis ($P + N$, $\mu_2 = 0.3\mu_1$ where P designates the *power law* model in the central core layer and N, the Newtonian model in the plasma layer) are compared with

(i) those of single layered Newtonian fluid (N, $\mu = 0.035$),
(ii) those of a single layered Power law model (P, $\mu = 0.1167$),
(iii) the results of the two-layered model case of Newtonian fluid ($N_1 + N_2$, $\mu_2 = 0.3\mu_1$, $\mu_1 = 0.035$),
(iv) those of a two–layered model case for a normal artery ($P + N$, $\tau_m = 0$),
(v) those for the rigid wall i.e. by disregarding the vessel wall flexibility.

Figure *2a* illustrates the results for the velocity profile of the core fluid at a specific locations for *z* — 15 mm for three different time periods. Two more curves corresponding to the same critical location are also plotted in the present figure at *t* = 0.5 *s* just by disregarding the presence of stenosis in one and by withdrawing wall motion in another. The number within the parenthesis appearing in the four top curves indicate that the respective results are obtained by dividing them with the specified numbers. The curves are all found to be diminishing from their maximum

at the axis as one moves away from it and finally they approach their minimum values at the interface between the central core and the plasma where the core velocity merges completely with the velocity of plasma. One notable feature is that the diminishing rate of the core velocity appears to be considerably higher in the case of a normal artery (r_m = 0) than that for a constricted one corresponding to a critical location where the artery assumes its maximum constriction. The deviation of the results thus obtained clearly estimates the effect of arterial stenosis on the velocity profile of the core fluid. The core velocity is reduced considerably when the motion of the arterial wall is totally withdrawn from the present system as evident from the comparison of the second and third curves from the bottom plotted for £=0.5 s. Thus the distensibility of the arterial wall also possesses a significant effect on the velocity of the core fluid. Regarding their variations with time indicating unsteadiness, one may note that the core velocity gets enhanced its magnitude with increasing time without altering the nature of the profile.

The velocity profile of the peripheral plasma layer corresponding to the same critical site as mentioned above has been shown in Figure *2b* for different time periods. A sharp diminishing trend of the results unlike those of Figure *2a* may be attributed to the close presence of the stenosis together with the viscosity of the fluid in this part under study. Here the curves do diminish at a relatively high rate as one proceeds towards the arterial wall surface and eventually they approach a minimum value (zero) on the wall surface. Although the presence of arterial constriction causes a sizeable deviation of the onset velocity but this gradually diminishes and finally disappears on the arterial wall surface. The wall distensibility does not however influence the plasma velocity profile much unlike the velocity profile of the core fluid as evident from the pair of closed adjacent curves of the present figure.

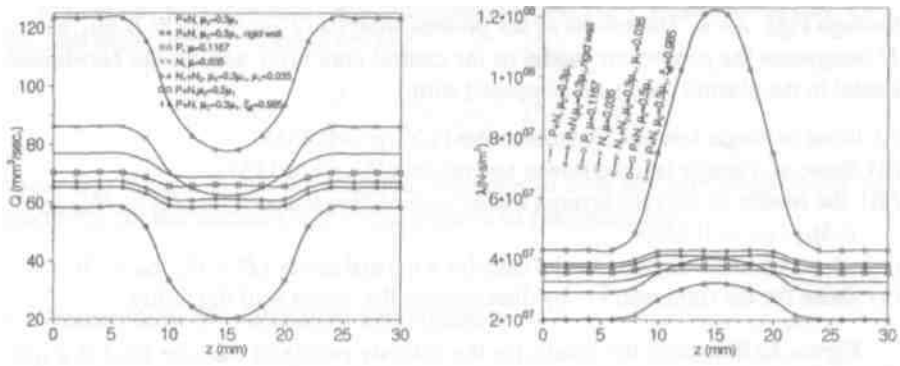

Figure 3. Distribution of the (*a*) rate of flow and (*b*) the resistance to flow at $t = 0.5\,sec$ $(\tau_m = 0.2a, \xi_\beta = 0.95,\ \mu_1 = 0.1167)$.

Figure *3a* records the distribution of the flow rate over the entire arterial segment at a particular instant of $t = 0.5$ 5, where various cases depending on the viscosity of the fluid in different situations have been explored. All the curves follow the general feature that the flow rate diminishes at the onset of the stenosis until the maximum constriction and thereafter increases symmetrically along the diverging section of the stenosis, that is, the flow rate curves become perfectly symmetrical about the maximum constriction site of z = 15 *mm* only in the stenotic region. However, they keep relatively higher values in the non-constricted portions of the arterial segment under study. One may note that the flow rate is reduced significantly in the absence of any arterial wall motion and thus the effect of wall distensibility can be easily quantified through direct comparison of the relevant curves of the present figure. The flow rate is further reduced drastically when the streaming blood of the artery is treated as a single non-Newtonian fluid (Power law) with different viscosity *(m* = 0.1167). However, the consideration of a single homogeneous Newtonian fluid with viscosity *fi* = 0.035 yields considerable enhancement of the distribution of the flow rate and hence the viscosity of the fluid representing blood plays a key role in the flux distribution. The flow rate appears to be all time higher in the case of two-layered Newtonian fluid fluids with different viscosity, the present figure also includes the corresponding results for a two-layered fluid by reducing the peripheral plasma thickness showing a sizeable reduction of the flow rate over the entire arterial segment under consideration. Perhaps it would be of some importance to note from the general characteristics of the curves that the flow rate enhances or reduces to some extent with the arterial length in the constricted region depending upon whether the arterial cross-section increases or decreases respectively.

The results for the resistances to flow or the impedances experienced by the non-homogeneous blood distributed over the entire arterial segment at t = 0.5 *s* are displayed in Figure *3b* where all possible cases for homogeneous-nonhomogeneous-Newtonian -non-Newtonian fluids with various viscosities are well explored. Unlike the behaviour of the flow rate, the resistive impedances get enhanced at the onset of the stenosis from relatively higher values in the non-stenotic portion until its maximum constriction and thereafter diminishes sharply as the constriction assumes a minimum followed by a linear path outside the stenotic region. It is evident from the results that the flowing blood experiences higher resistances to flow when the arterial wall is treated to be rigid and hence the effect of wall motion on the resistive impedances can be quantified. Studying all the results of Figure 3 one can conclude that since the resistive impedances are inversely proportional to the flow rate, the representative curves of the present figure appear to be almost reciprocal to those of the flow rates. It is important to note that the flow of a single homogeneous Newtonian fluid experiences maximum impedances and the distribution is found to be more than that for a two-fluid flow in general and for a single non-Newtonian flow, in particular. Moreover, the effect of the peripheral plasma thickness on the resistive impedances appears to be significant and hence its contribution should be taken into account in the realm of the flow characteristics of blood.

Figure *4a* shows the distribution of the wall shear stress over the entire stenosed arterial segment at the same instant of time. The curves of the present figure represent the respective wall shear stress corresponding to a variety of cases mentioned earlier with distinguishable marks. All the curves barring the bottom most one at-

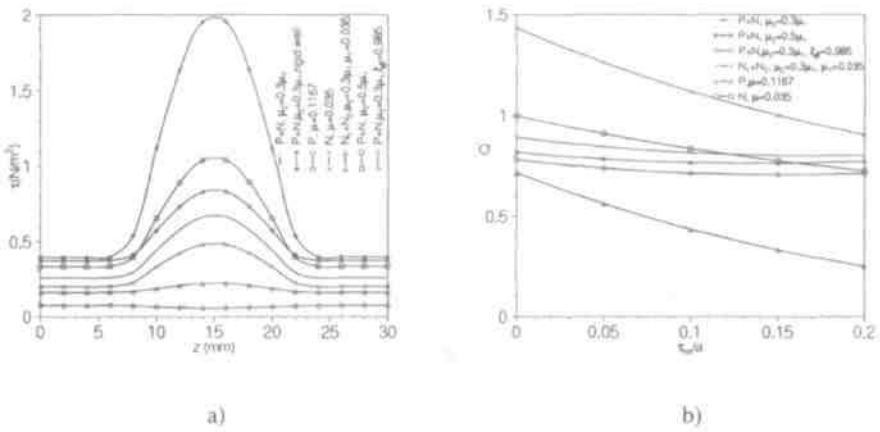

a) b)

Figure 4. a) distribution of wall shear stress at $t = 0.5sec$ ($\tau_m = 0.2a, \mu_1 = 0.1167, \xi_\beta = 0.95$) b) distribution of dimensionless flow rate for $t = 0.5sec$ at $z = 15mm(\xi_\beta = 0.95, \mu_1 = 0.1167, l_0/L = 0.5)$.

tain their peaks at the critical site of the maximum arterial constriction. The non-stenotic portions are however being distributed with relatively lower stress values. The stress developed on the arterial wall surface is observed to enhance considerably if one completely disregards the wall motion. A further enhancement of the stress appears more in the stenotic region than in the nonstenotic region when the plasma-viscosity of the two-layered fluid is slightly increased as indicated in the relevant curve of the present figure. If one treats the streaming blood to be a single plasma Newtonian fluid, then the wall shear stress is found to drop significantly more in the constricted zone than in the unconstricted region unlike other curves while a single non-Newtonian fluid model causes the stress to increase substantially lying below the range of stress values corresponding to the two-layered fluid. However, a reduction of the wall shear stress distribution is noted for a two-fluid Newtonian model with different viscosity. All these results mentioned here correspond to a specific plasma-thickness of 0.05 but the moment it is reduced slightly to 0.015, the wall shear stress gains all time higher values over the entire arterial segment. The present stress distribution plays a very important role in detecting the aggregation sites of platelets as mentioned in [9] that the growth and the deterioration of the endothelial cells of the arterial wall are closely related to the generation of shear stress on the arterial walls.

The behaviour of the dimensionless flow rate with severity of the stenosis present in the arterial lumen at specific location where the stenosed artery assumes its constriction maximum is exhibited in Figure *4b*. The present two-fluid model with a viscosity ratio of plasma to core $(\frac{\mu_2}{\mu_1} = 0.3)$ experiences a gradual decay of the flow rate with the increase in the severity of the stenosis, which gets slightly perturbed with considerable reduction in magnitudes when the viscosity ratio is raised to 0.5,

that is, when the plasma viscosity is increased. The rate of declination of the curve appears to be quite rapid if the viscosity of the core fluid is diminished considerably as observed from the topmost curve of the present figure. On the other hand, consideration of a single fluid model yields a sharp decline of the flow rate with lower magnitudes when the viscosity of the streaming blood is reduced from 0.1167 to 0.035 and the effect of viscosity together with severity of the stenosis on the flow rate can be estimated thereby. The reduced peripheral plasma thickness causes a reduction of the flow rate which is slightly perturbed with the change of severity of the stenosis.

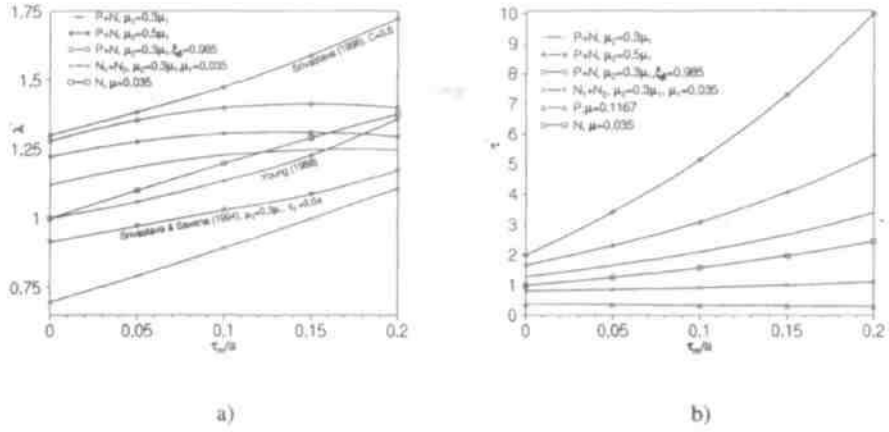

Figure 5. Distribution of (a) dimensionless resistance to flow and (b) dimensionless wall stress for $t = 0.5sec$ at $z = 15mm$ ($\xi_\beta = 0.95, \mu_1 = 0.1167, l_0/L = 0.5$).

For the purpose of making a comparative study with the existing results relevant to this domain in order to validate the model under consideration, the results of Figure 5a illustrate the behaviour of the resistive impedances with severity of the stenosis at its maximum constriction site. The severity of the constriction can be visualized by increasing the height of the stenosis. All the results of the present study show that the resistive impedances keep on increasing with the increasing height of the stenosis, that is, more the severity of the stenosis larger is the resistive impedance experienced by the flowing blood in all the cases indicated in the figure. The corresponding results of Young [23], Srivastava and Saxena [19] and Srivastava [18] are also reproduced in the present figure which do agree qualitatively and, to some extent, quantitatively with the present results. Any quantitative difference of results from the previous studies may be responsible owing to the difference in the present geometry of the constriction, the incorporation of the arterial wall motion and to the unsteadiness of the present flow considerations. The present results also include the significant effect of the peripheral plasma thickness on the resistive impedances varying directly with the stenosis-severity. Thus one may conclude that if constriction keeps on growing, then resistance grows up fast, with or without the arterial motion. It is, however, worth mentioning that the present theoretical model possesses a poten-

tial improvement over the analytical investigations carried out by them as mentioned above.

Figure *5b* exhibits the behaviour of the non-dimensional wall shear stress experienced by the flowing blood in various situations with different sizes of the stenosis at the same critical location of *(z* = 15 *mm)* maximum constriction site. The notable feature is that the shear stress gets enhanced appreciably with the severity of the stenosis following an exponential path unlike the nature of resistive impedances as shown in Figure 5a. One may observe that when the viscosity of the plasma fluid is increased, the wall shear stresses do increase significantly while they diminish appreciably with the reduction of the core fluid viscosity for a two-layered fluid model representing blood. However, in the case of a single homogeneous fluid, the reduction of the fluid viscosity causes the shear stress to enhance considerably, which is in contrast to the findings of a two-layered model. The further enhancement of the wall shear stress for plasma thinning is also recorded in the present figure so as to validate the importance of the present two-layered model under consideration.

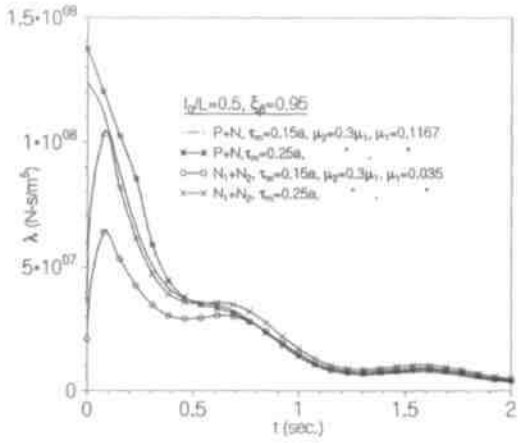

Figure 6. Variation of the resistance to flow with time for $z = 15\,mm$.

The variation of the resistive impedances with time spanned over a few cardiac cycles at the critical location 2 = 15 *mm* of the stenosed artery is included in the concluding Figure 6 for two different severity of the stenosis having length equal to half the length of the arterial segment. The results of impedances are represented by four distinct curves of which the top two correspond to the present two-fluid model (consisting of a non-Newtonian core and a Newtonian plasma) with different severity of the stenosis while the bottom two represent a different two-layered model of Newtonian fluids with two specific stenosis-severity. The nature of the top two curves is analogous where the resistive impedance drops from its maximum value at the onset of the cardiac cycles till time *t* = 0.5 *s* followed by a slower rate of decrease for the rest of the cardiac cycles. The deviation of the results of these two curves

clearly indicate the effect of severity of the stenosis on the resistive impedances and that appears during the first cardiac cycle only. A little different feature is however observed from the bottom pair of curves. The peak impedance appears to be shifted a little to the right at the onset of the first cardiac cycle and then it drops down with undulating pattern for the rest of the cycles considered here. Once again, the severity of the stenosis caused an increase of the resistive impedance. Studying all the results of the present figure, one may note that even though the resistive impedances appear to have significant differences towards the first cardiac cycle but those gradually die out with advancement of time within a few cardiac cycles.

The significance of the present analysis of the two-layered model of *power law* fluid can now be understood well from the discussion above. Through the numerical evaluations obtained in the analysis for various values of the parameters involved, it may be remarked that the effects of peripheral layer viscosity, the peripheral layer thickness, presence of peripheral layer and the non-Newtonian rheology of the flowing blood on the flux, the resistance to flow and the wall shear stress are quite significant. The results of the present study also agree qualitatively well with some existing ones. Therefore the present mathematical model bears the potential to predict the main characteristics of the physiological flows under in vivo situation and would certainly be of considerable interest in biomedical applications which in turn validates the applicability of this model.

References

[1] G. Bugliarello and J. Sevilla. Velocity distribution and other characteristics of steady and pulsatile blood flow in fine glass tubes. *Biorheology,* 7, 85 - 107, 1970.

[2] A. C. Burton. *Physiology and Biophysics of the Circulation, Introductory Text.* Year Book Medical Publisher, Chicago, 1966.

[3] C. G. Caro, T. J. Pedley, R. C. Schroter and W. A. Seed. *The Mechanics of the Circulation.* Oxford University, 1978.

[4] S. Chakravarty. Effects of stenosis on the flow behaviour of blood in an artery. *J. Engng. ScL,* 25, 1003 - 1016, 1987.

[5] S. Chakravarty and A. Dutta. Effects of stenosis on arterial rheology through a mathematical model. *Math. Comp. Modelling,* 12, 1601 - 1612, 1989.

[6] S. Chakravarty and A. Dutta. Dynamic response of stenotic blood flow in vivo. *Math. Comp. Modelling,* 16, 3 - 20, 1992.

[7] G. R. Cokelet. The rheology of human blood. In: *In Biomechanics.* Prentice-Hall, Englewood Cliffs, N. J., 63 - 103, 1972.

[8] G. R. Cokelet and H. L. Goldsmith. Decreased haemodynamic resistance in the two-phase flow of blood through small vertical tubes at low flow rates. *Circ. Res.,* 68, 1 - 17, 1991.

[9] D. L. Fry. Acute vascular endothelial changes associated with increased blood velocity gradients. *Circulation Res.,* 22, 165 - 197, 1968. [10] K. Imaeda and F. O. Goodman. Analysis of nonlinear pulsatile blood flow in arteries. /. *Biomech.,* 13, 1007 - 1022, 1980. [11] P. K. Mandal. An unsteady analysis of nonlinear two-layered 2D model of pulsatile flow through stenosed arteries. *Math. Model. Analysis,* 8(3), 229 - 246, 2003.

[12] W. R. Milnor. *Hemodynamics.* Williams and Williams, Baltimore, 1982.

[13] J. C. Misra and S. Chakravarty. Flow in arteries in the presence of stenosis. *J. Biomech.*, 19,907-918. [14] R. N. Pralhad and D. H. Schultz. Two-layered blood flow through stenosed tubes for different diseases. *Biorheology*, 25, 715 - 726, 1988. [15] M Sharan and A. S. Popel. A two-phase model for flow of blood in narrow tubes with increased effective viscosity near the wall. *Biorheology*, 38, 415 - 428, 2001. [16] J. B. Shukla, R. S. Parihar and B. R. P. Rao. Effects of peripheral layer viscosity on blood flow through the artery with mild stenosis. *Bull. Math. Biol.*, 42, 797 - 805, 1980b. [17] J, B. Shukla, S. Parihar, R and B . R. P Rao. Effects of stenosis on non-newtonian flow of the blood in an artery. *Bull. Math. Biol*, 42, 283 - 294, 1980a. [18] V. P. Srivastava. Two-phase model of blood flow through stenosed tubes in the presence of a peripheral layer: Applications. *J. Biomech.*, 29, 1377 - 1382, 1996. [19] V. P. Srivastava and M. Saxena. Two-layered model of Casson fluid flow through stenotic blood vessels: applications to the cardiovascular system. *J. Biomech.*, 27, 921 - 928, 1994. [20] H. W. Thomas, R. J. French, A. C. Groom and S. Rowlands. The flow of red cell suspensions through narrow tubes. In: *Proc. IVth. Int. Cong. Rheology*, volume 4, Interscience, **New** York, 381-391, 1965. [21] G.B.Thurston. Plasma release-cell layering theory for blood flow. *Biorheology*, 26, 199-214, 1989. [22] J. R. Womersley. Oscillatory motion of a viscous liquid in a thin-walled elastic tube-I: The linear approximation for long waves. *Phil. Mag.*, (Ser.7), 199 - 221, 1955. [23] D. F. Young. Effect of a time-dependent stenosis of flow through a tube. *J. Engng. Ind.*, 90, 248-254, 1968. [24] D. F. Young. Fluid mechanics of arterial stenosis. *J. Biomech. Engng. Trans. ASME*, **101,** 157-175, 1979.

Nestacionaraus dvisluoksnio pulsuojančio kraujo srauto tekėjimas esant stenozei lanksčioje arterijoje skaitinis modeliavimas: periferinio sluoksnio klampumo efektai

S. Chakravarty, P.K. Mandal, A. Mandal

Straipsnyje nagrinėjamas kraujo srauto tekėjimas esant stenozei. Nagrinėjamas dvisluoks-nis kraujo tekėjimas. Arterija modeliuojama kaip vamzdis su elastinėmis sienelėmis. Kraujo srauto nestacionarumą sukelia širdies veikla. Skaitinis sprendinys randamas baigtinių skirtumų metodu. Atlikta kokybinė skaitinių sprendinių analizė iliustruojanti greičių, srautų, sienelės įtampų priklausomybę laike. Skaitiniai rezultatai pakankamai gerai patvirtina eksperimentinius duomenis.